Electronic Supplementary Information

On the role of torsional dynamics in the solid-state fluorescent properties of a new bifluorene-tetracarboxylic acid and its supramolecular assemblies: a structural and TD-DFT investigation

Enrico Podda,[a,b] Massimiliano Arca,[a] Anna Pintus,[a] Vito Lippolis,[a] Claudia Caltagirone,[a] Simon J. Coles,[d] James B. Orton,[d] Guido Ennas,[a] Giacomo Picci,[a] Robert P. Davies,*[c] M. Carla Aragoni*[a]

[a] *Dipartimento di Scienze Chimiche e Geologiche, Università degli Studi di Cagliari, Cittadella Universitaria, SS. 554 bivio Sestu, 09042 Monserrato – Cagliari, Italy.*
[b] *Centro Servizi di Ateneo per la Ricerca, Università degli Studi di Cagliari, Cittadella Universitaria, SS. 554 bivio Sestu, 09042 Monserrato – Cagliari, Italy.*
[c] *Department of Chemistry, Imperial College London, White City Campus, 80 Wood Lane, London W12 0BZ, United Kingdom.*
[d] *UK National Crystallography Service, School of Chemistry, Faculty of Engineering and Physical Sciences, University of Southampton, SO17 1BJ, United Kingdom.*

Email: aragoni@unica.it
r.davies@imperial.ac.uk

Table of Contents

Scheme S1 Different coordination modes of $\mathbf{L}^{4-}$: I) chelating (κ^2O); II) chelating/bridging (μ-oxo-1κ^2O-2κ^1O), III) bridging (μ-oxo-1κ^1O, 2κ^1O).

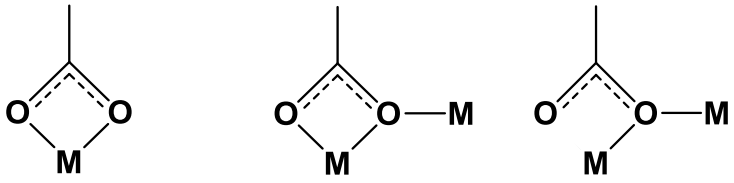

I **II** **III**

Figures

Fig. S1 Asymmetric unit of **1c**. Thermal ellipsoids are drawn at 50% probability level.

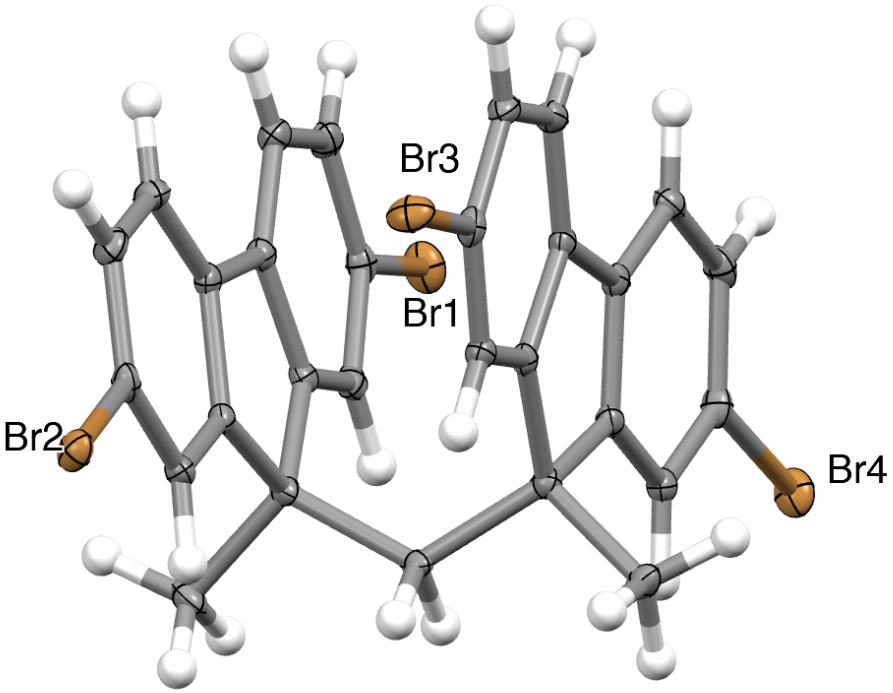

Fig. S2 Crystal structure of **1c**: intra- and intermolecular π-π interactions; hydrogen atoms omitted for clarity.

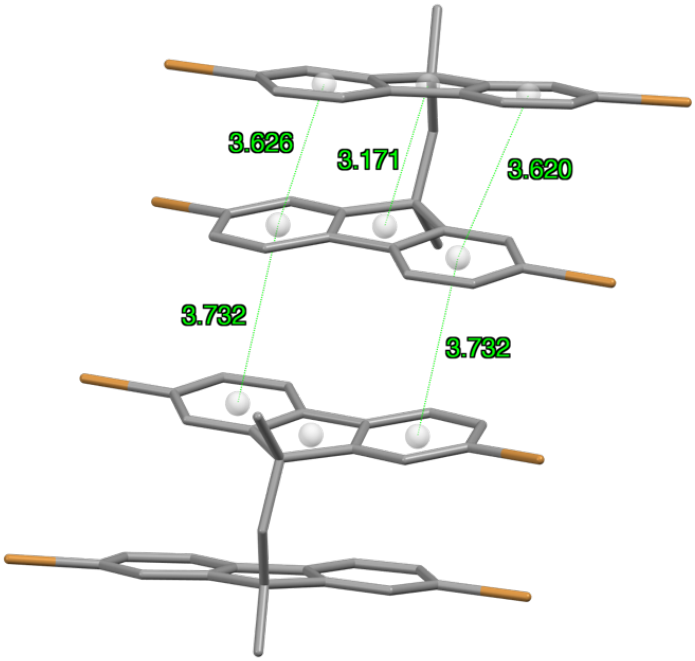

Fig. S3 Packing diagram of **1c** along *a* axis. H atoms are omitted for clarity. Inter-molecular centroid distances 3.73 Å, Br···Br contacts of 3.62 and 3.63 Å.

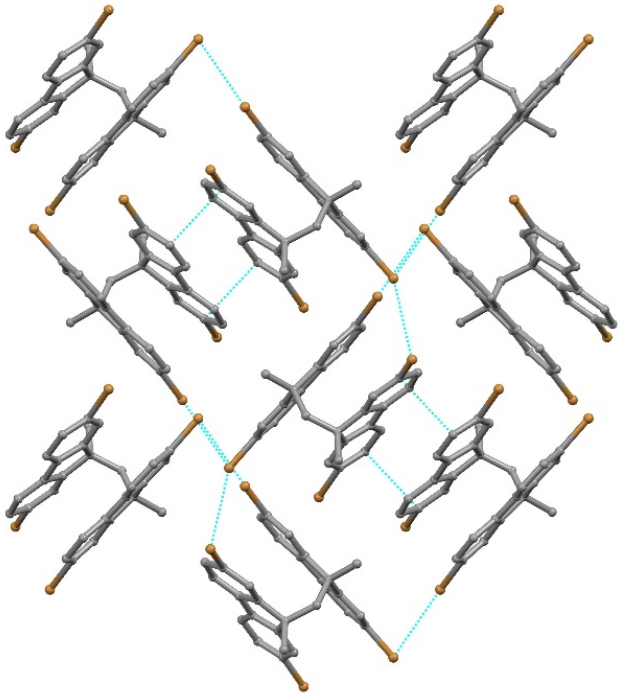

Fig. S4 Packing view of the H_4**L** chains along the 100 direction. Hydrogen bonding interactions are labelled accordingly to Table S1. Aryl protons not involved in showed interactions have been omitted for clarity reasons.

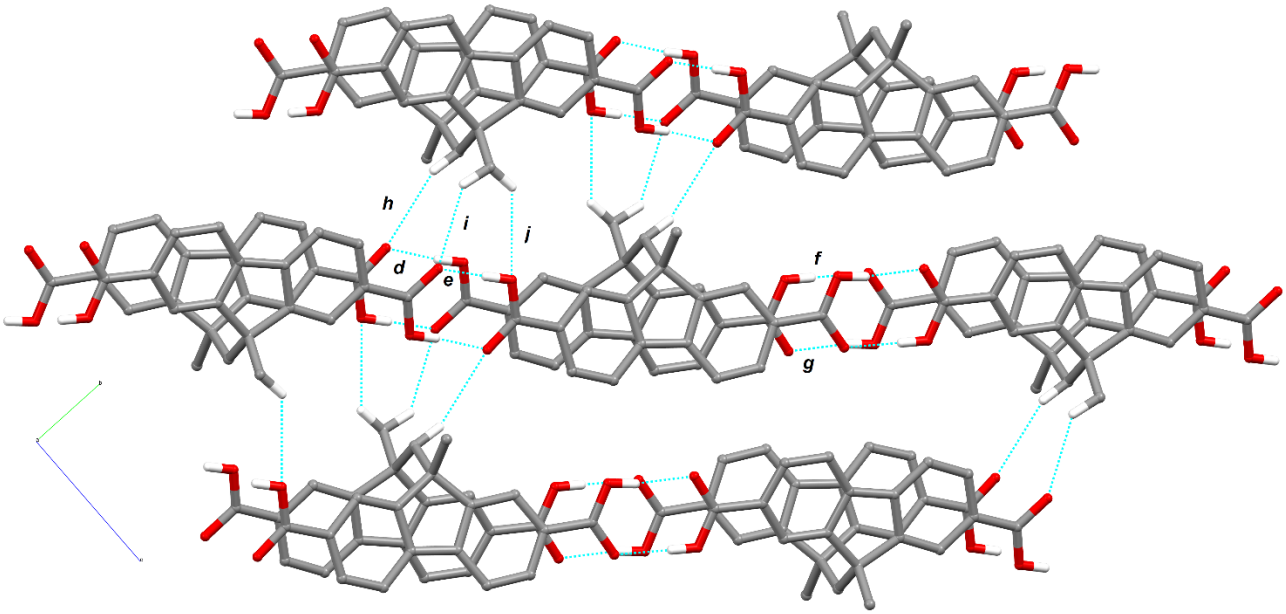

Fig. S5 Intermolecular hydrogen bonding in the crystal structure of **2**. Interactions are labelled according to Table S5. Only interacting H atoms are shown for clarity.

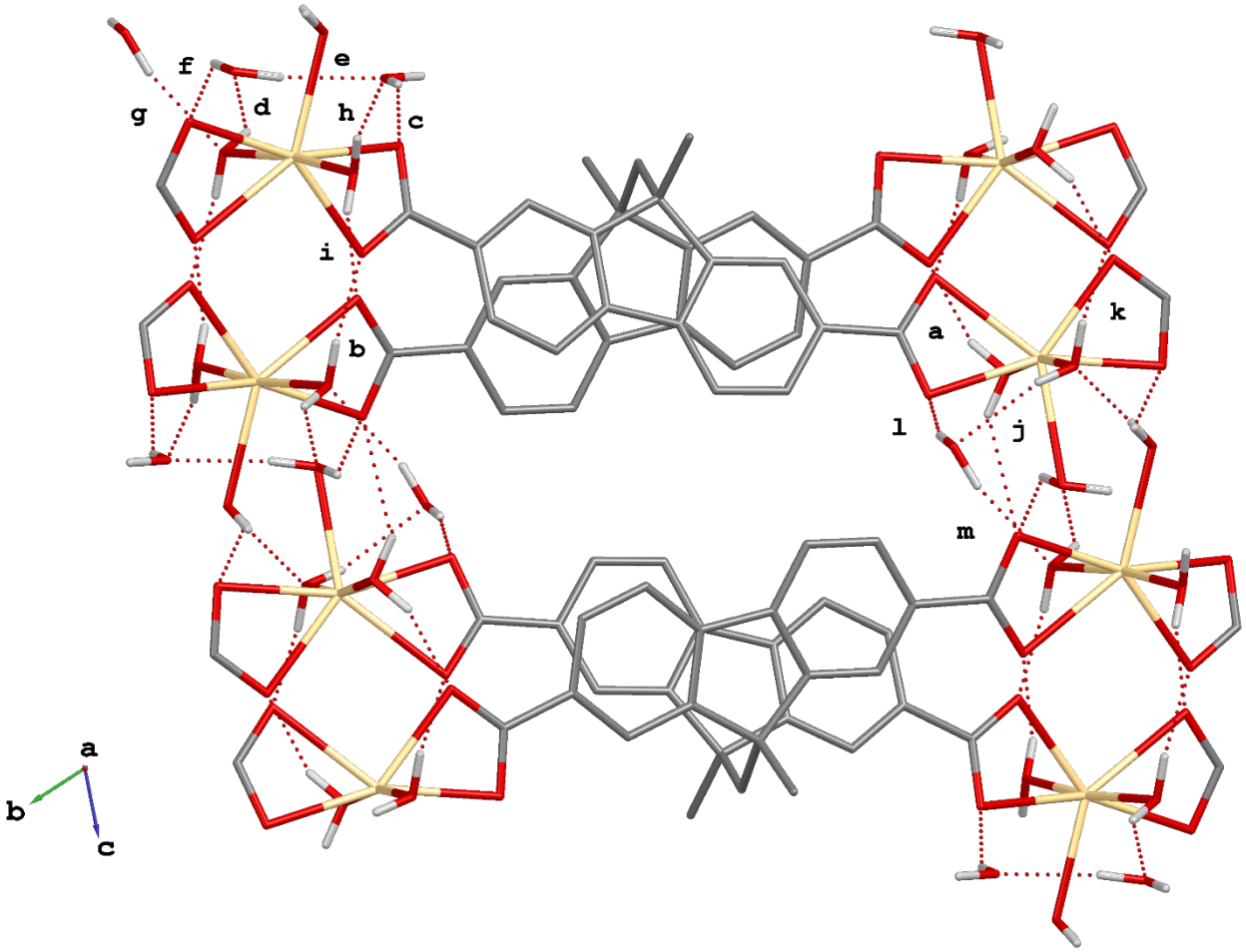

Fig. S6 Packing diagrams of **2** along the *a* and *c* axis. Interactions are labelled according to Table S5. Only interacting H atoms are shown for clarity.

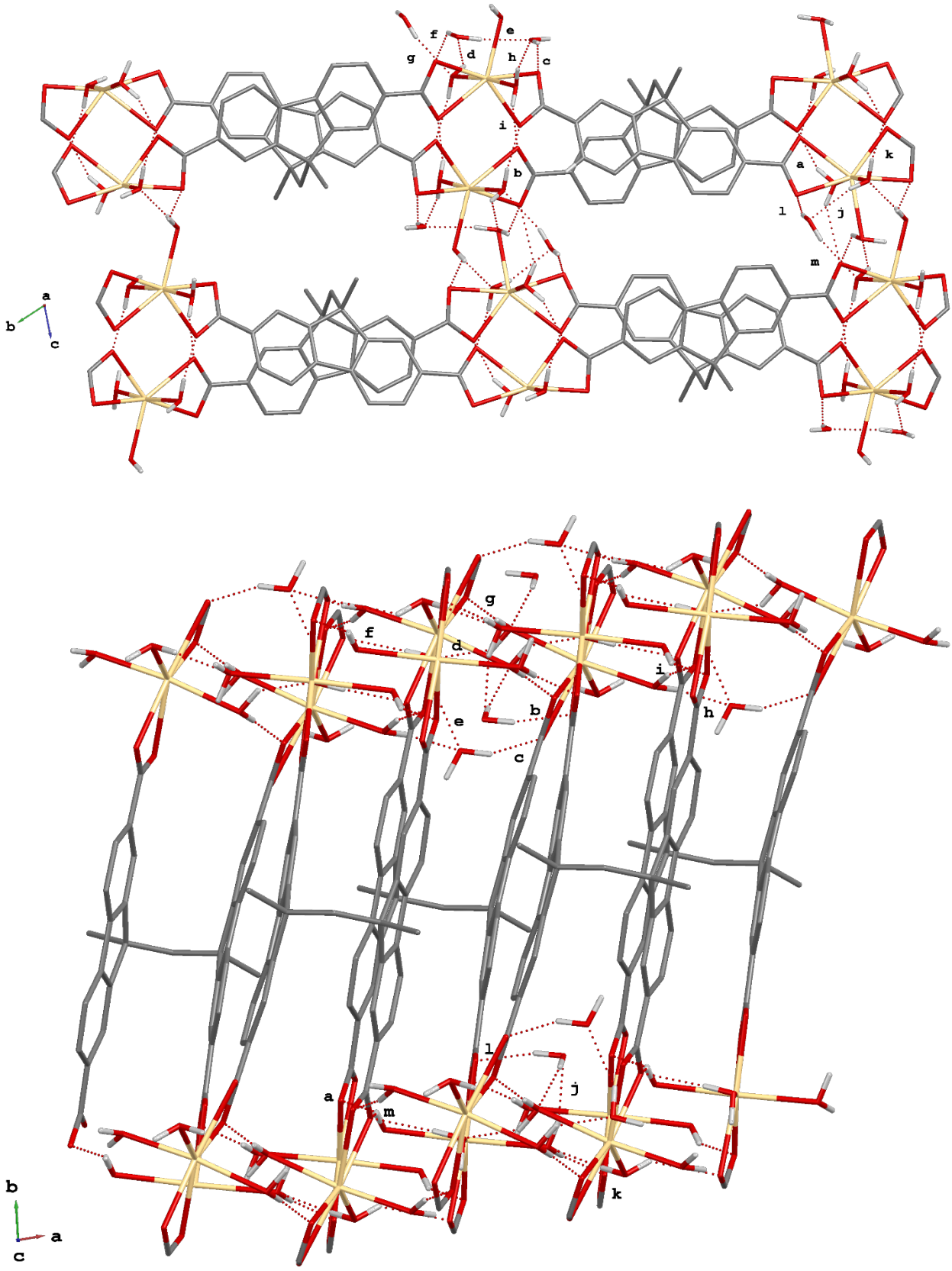

Fig. S7 PXRD analysis: experimental patterns on the solvothermal reaction products between H_4**L** and $Cd(NO_3)_2 \cdot 4H_2O$ in a 1:2 molar ratio in a DMA/H_2O mixture (2:1 v/v) at 90 (green) and 120 °C (blue); simulated patterns from CIFs of compounds **2** (black), **3**(red), H_4**L**(magenta) are also shown for comparison.

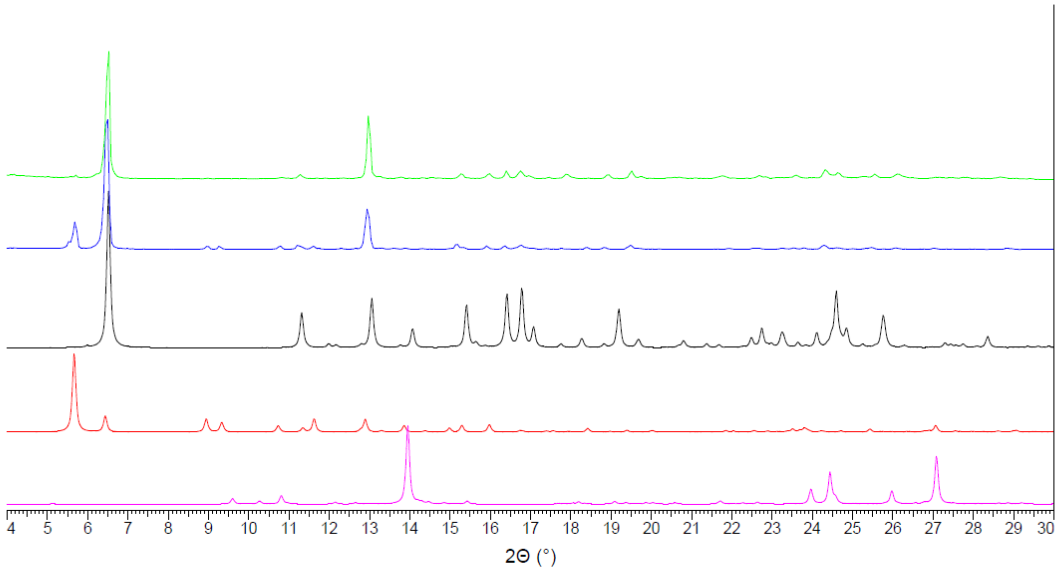

Fig. S8 DSC (left) and TGA (right) analysis of compound **2** (black) and of the mixture **2+3** (red).

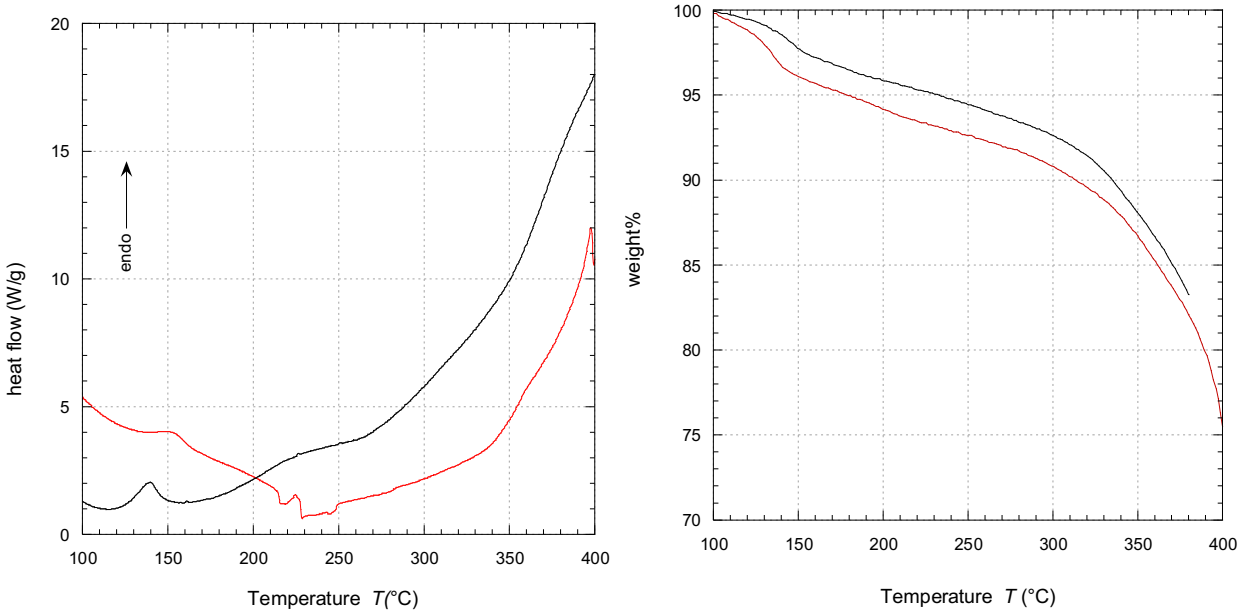

Fig. S9 Absorption (solid line) and emission (dashed line) spectra for H_4**L** measured in DMSO (left; [H_4**L**] = 10^{-5} M, λ_{ex} = 303 nm) and in the solid state (right; λ_{ex} = 372 nm).

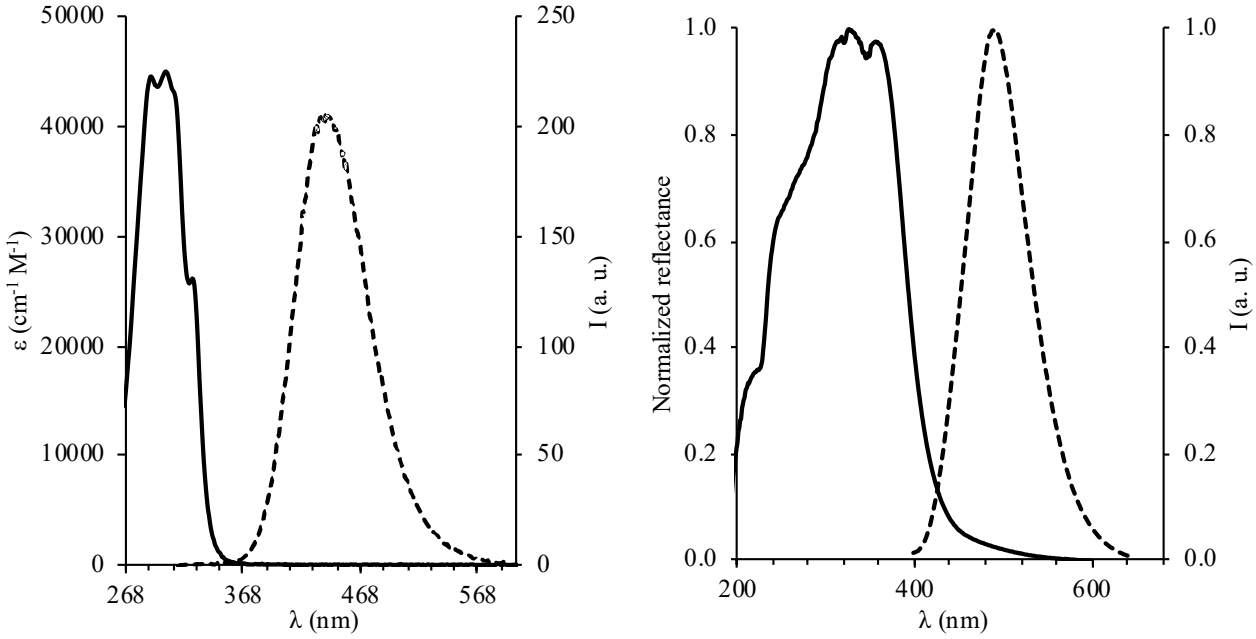

Fig. S10 Normalised solid-state diffuse reflectance spectra (200–600 nm) determined for H_4**L** (dark blue), compound **2** (green), and **2+3** (red).

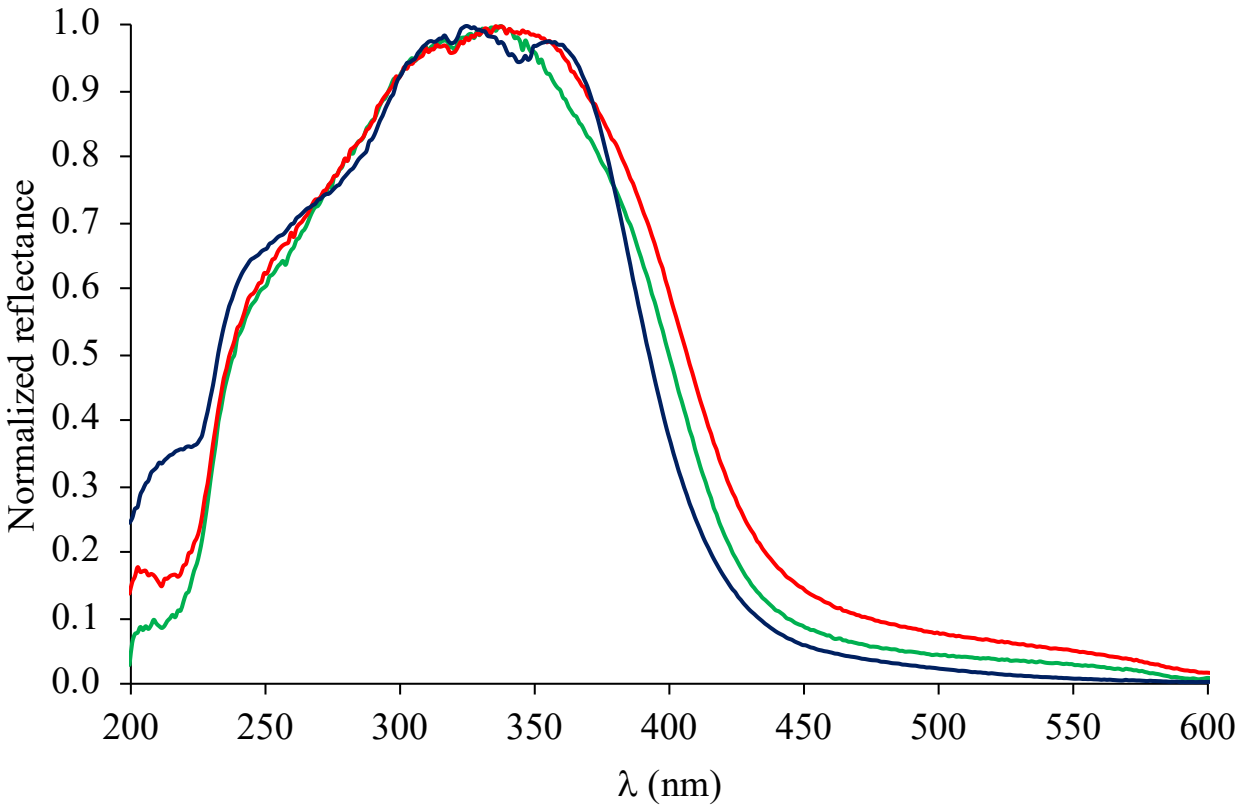

Fig. S11 Molecular orbitals isosurfaces calculated for H_4L in the gas phase at DFT level (PBE0//def2-SVP): HOMO–1 (MO #142; a), HOMO (MO #143; b), LUMO (MO #144; c), and LUMO+1 (MO #145; d). Cutoff value = 0.05 |e|. Carbon atoms are depicted in grey and oxygen atoms in red; hydrogen atoms omitted for clarity.

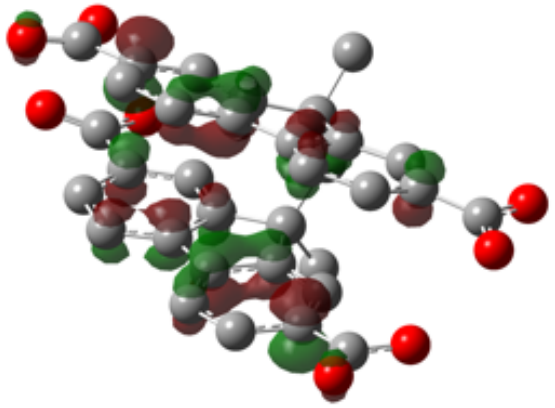

(a)

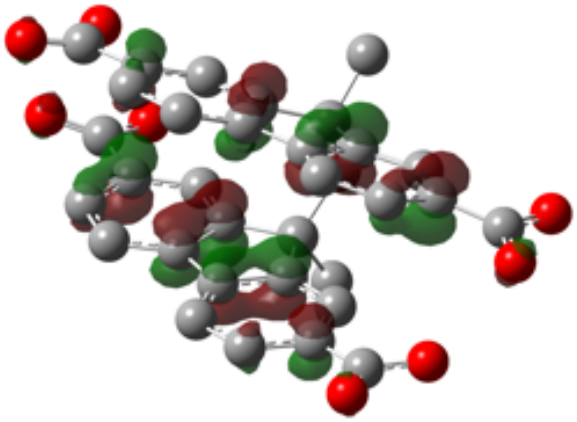

(b)

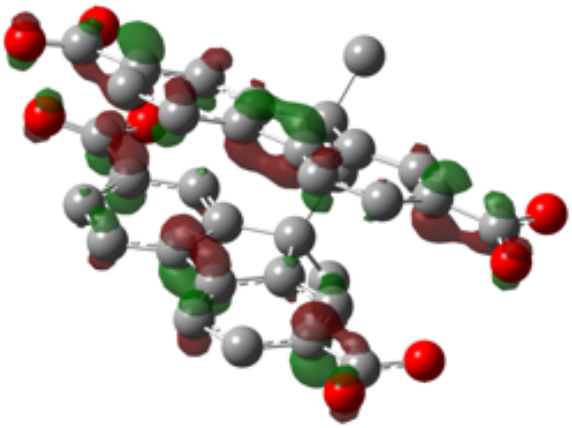

(c)

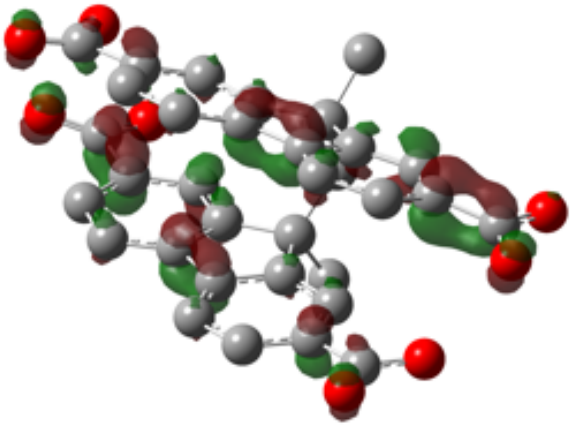

(d)

Fig. S12 Natural transition orbitals (NTOs) isosurfaces calculated for H_4L in the gas phase at TD-DFT level for transition 4. NTO #143 (particle, a) and NTO #144 (hole, b) exhibit the largest occupations (0.57) for ES #4. Cutoff value = 0.05 |e|. Carbon atoms are depicted in grey and oxygen atoms in red; hydrogen atoms omitted for clarity.

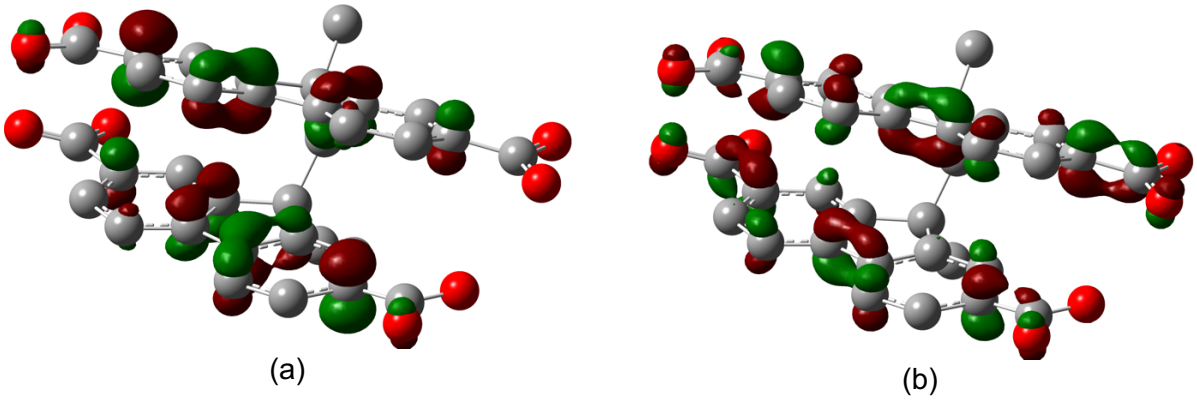

(a) (b)

Fig. S13 Molecular orbitals isosurfaces calculated for model complex 4 (a) in the gas phase at DFT level (PBE0//def2-SVP): HOMO–1 (MO #258; b), HOMO (MO #259; c), LUMO (MO #260; d), and LUMO+1 (MO #261; e). Cut-off value = 0.05 |e|. Carbon atoms are depicted in grey, cadmium ions in green, and oxygen atoms in red; hydrogen atoms omitted for clarity.

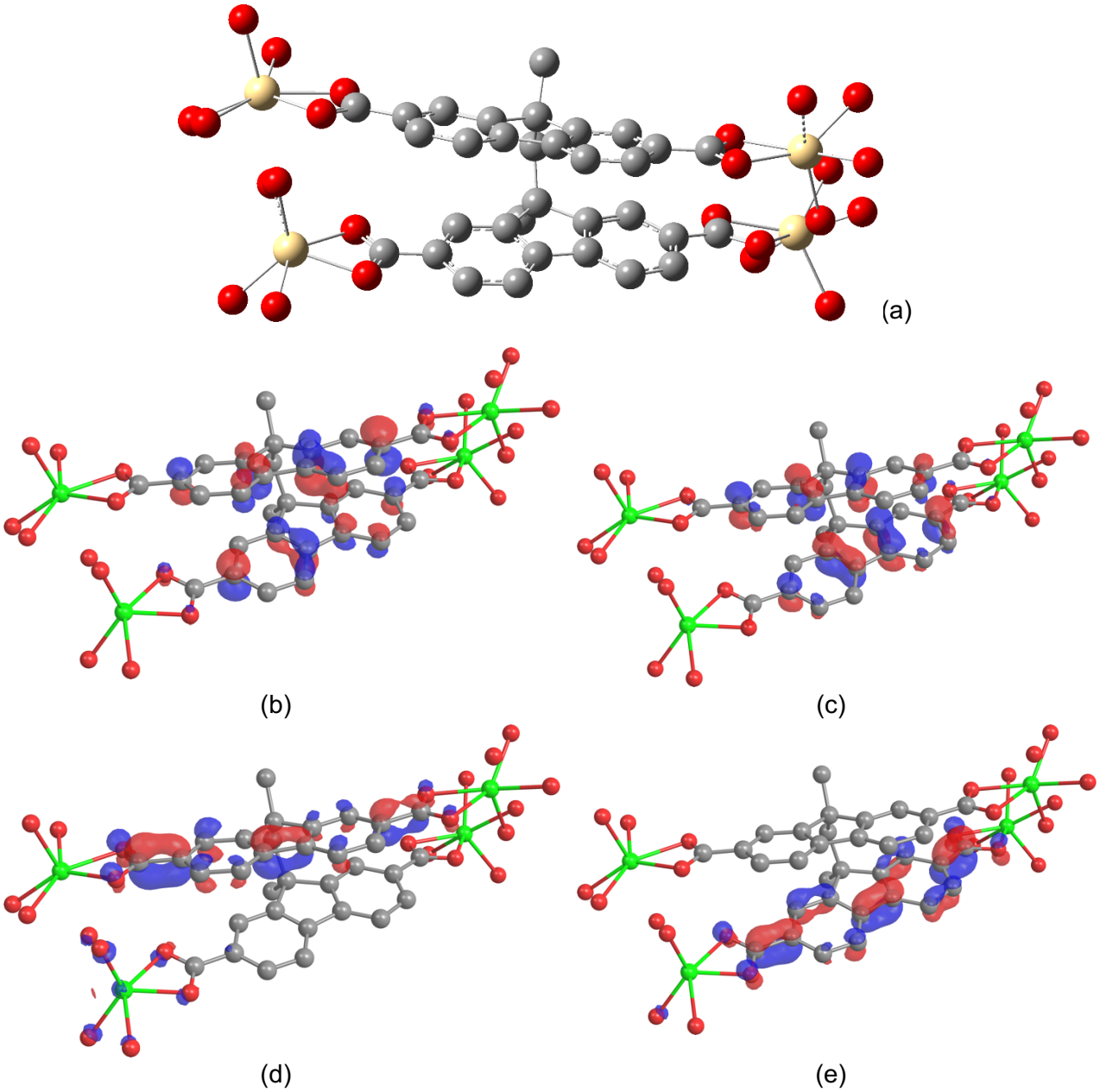

Fig. S14 Natural transition orbitals (NTOs) isosurfaces calculated for complex 4 in the gas phase at TD-DFT level for transition 4. NTO #259 (particle, a) and NTO #260 (hole, b) exhibit the largest occupations (0.52) for ES #4. Cutoff value = 0.05 |e|. Carbon atoms are depicted in grey and oxygen atoms in red; hydrogen atoms omitted for clarity.

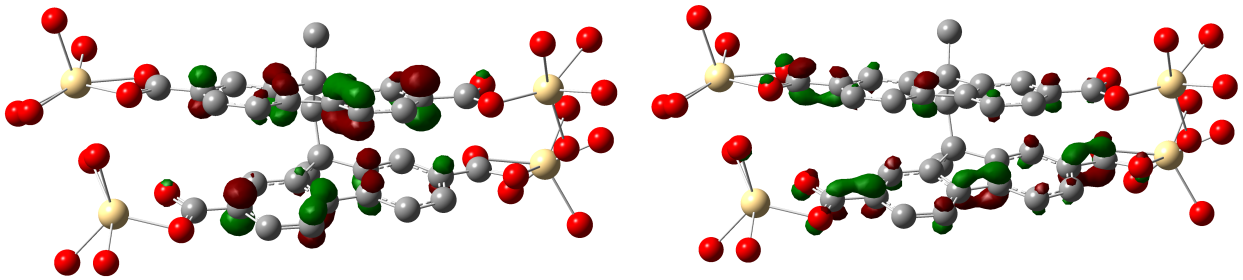

(a) (b)

Fig. S15 ^{1}H NMR (400 MHz, DMSO-d_6) of H_4**L**

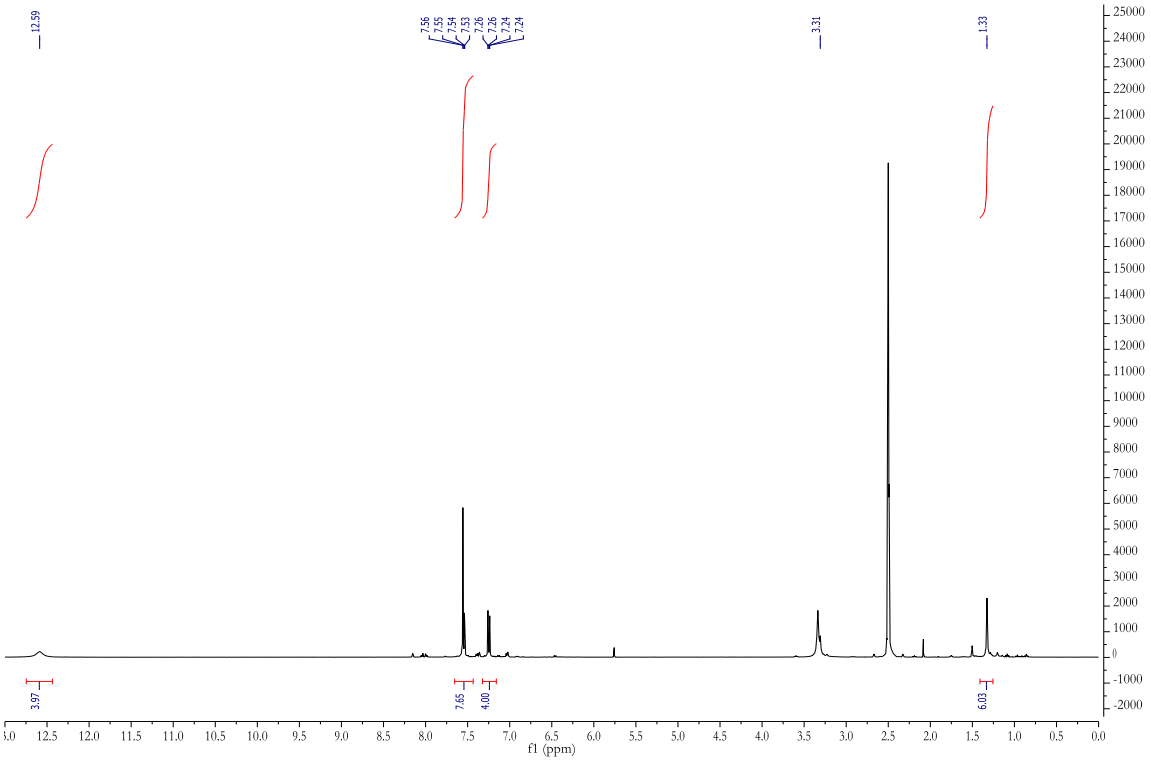

Fig. S16 ^{13}C{^{1}H} NMR (101 MHz, DMSO-d_6) of H_4**L**

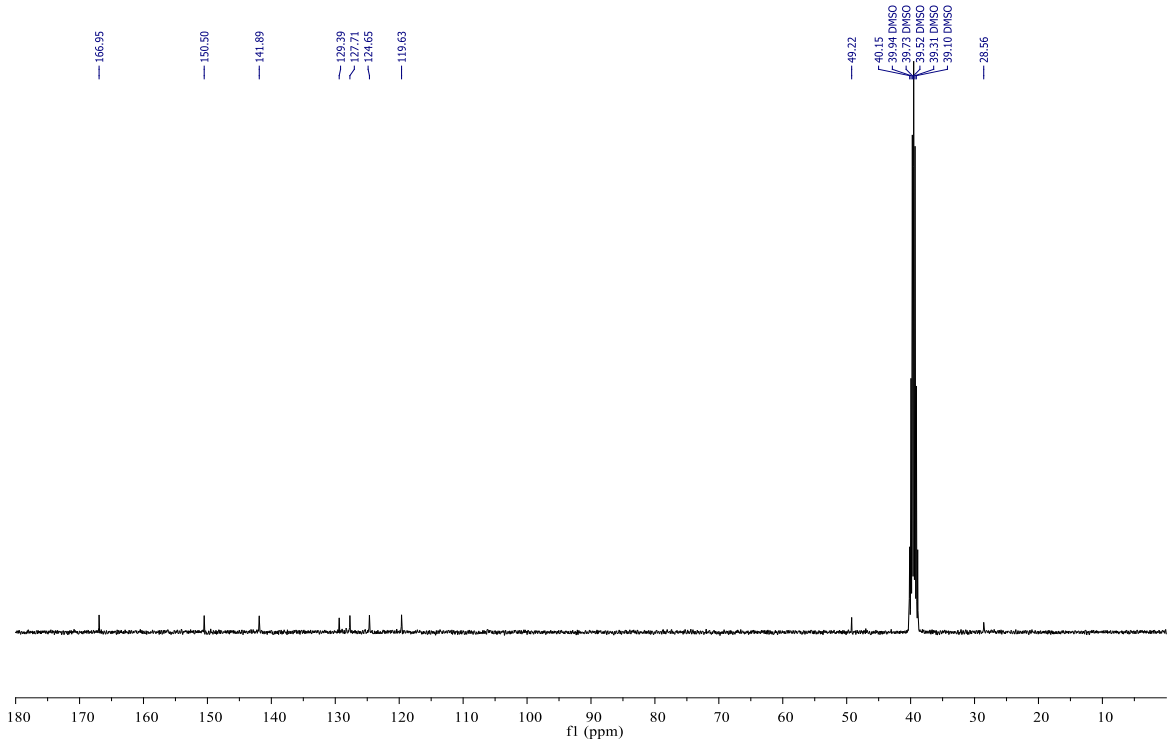

Fig. S17 ^{1}H-^{13}C HMQC of H_4**L** in DMSO-d_6

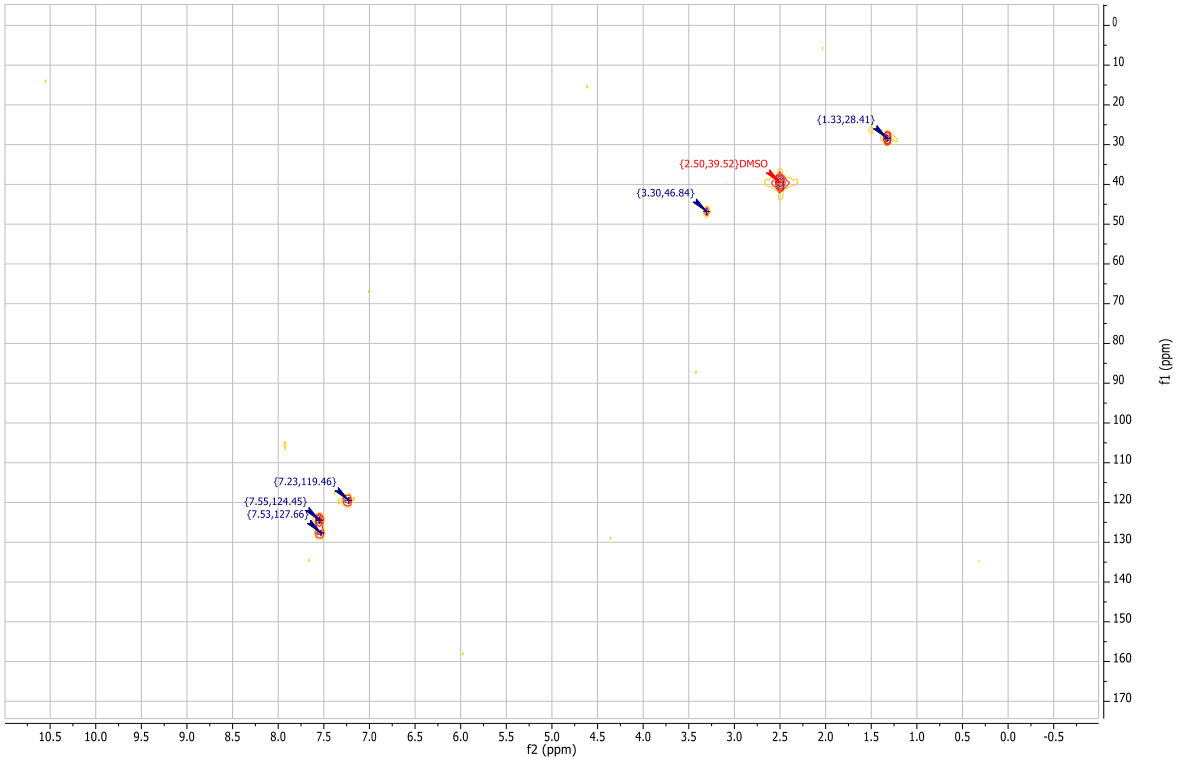

Fig. S18 TOF MS ES- of H_4**L**

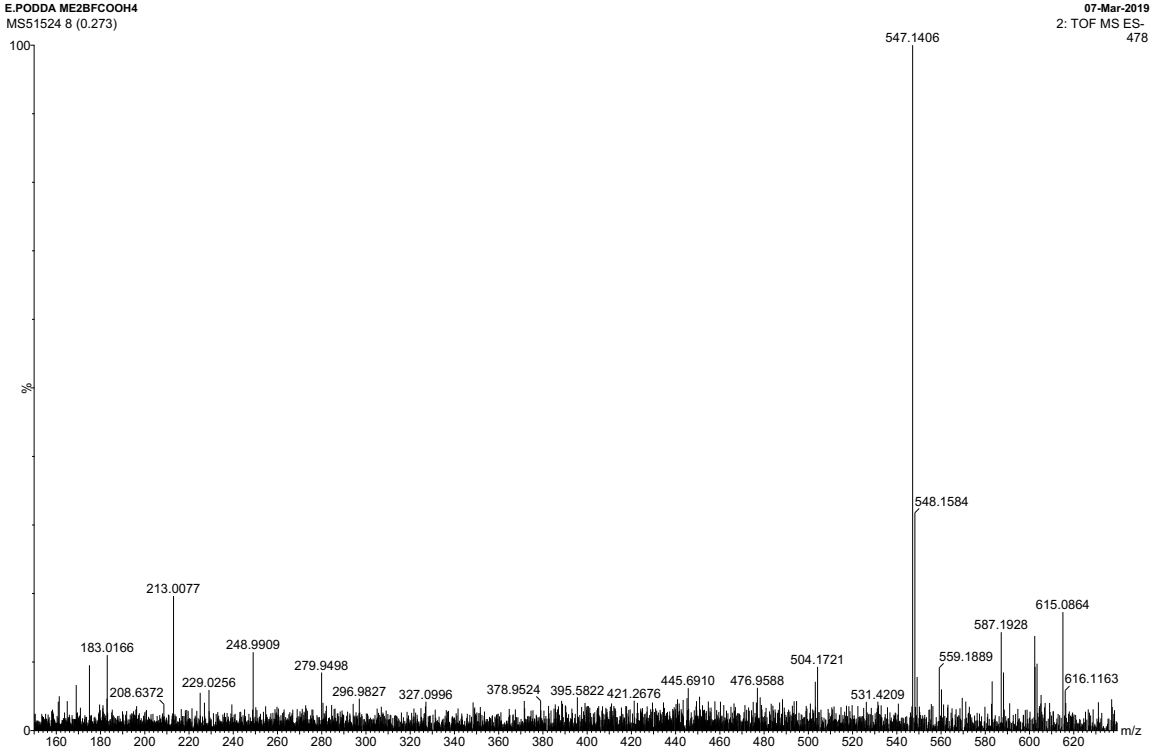

Tables

Table S1 Crystal data and structure refinement parameters for compounds **1c**, H_4**L**, **2,** and **3**.

	1c	H_4**L**	**2**	**3**
Formula	$C_{29}H_{20}Br_4$	$C_{33}H_{24}O_8$	$C_{33}H_{20}Cd_2O_8 \cdot 8H_2O$	$C_{33}H_{20}Cd_2O_8 \cdot 6H_2O$
$D_{calc.}$/ g cm^{-3}	1.896	1.454	1.808	1.649
μ/mm^{-1}	6.695	0.864	1.345	10.775
Formula Weight	688.09	548.52	913.42	823.34
Colour	colorless	colorless	colorless	colorless
Shape	cut block	block	plate	needle
Size/mm^3	0.34×0.23×0.12	0.09×0.06×0.03	0.08×0.07×0.03	0.06×0.01×0.01
T/K	100(2)	100(2)	100(2)	100(2)
Crystal System	monoclinic	triclinic	triclinic	orthorhombic
Flack Parameter	-	-	-	-0.005(12)
Hooft Parameter	-	-	-	-0.002(6)
Space Group	$P2_1/c$	P-1	P-1	$Cmc2_1$
a/Å	8.79840(10)	7.9080(6)	7.7940(3)	27.4335(7)
b/Å	16.7929(2)	9.8092(5)	14.7078(6)	18.9368(6)
c/Å	16.4790(2)	17.5752(9)	15.9272(6)	12.7660(5)
α/°	90	86.930(4)	67.884(4)	90
β/°	98.0820(10)	78.372(5)	86.175(3)	90
γ/°	90	69.784(6)	82.860(3)	90
V/Å^3	2410.60(5)	1252.89(14)	1677.93(12)	6632.0(4)
Z	4	2	2	8
Z'	1	1	1	1
Wavelength/Å	0.71075	1.54184	0.71075	1.54184
Radiation type	MoK_α	Cu K_α	MoK_α	Cu K_α
Θ_{min}/°	2.338	2.567	2.390	2.835
Θ_{max}/°	27.483	68.251	27.484	68.243
Measured Refl's.	54497	18130	38564	29109
Indep't Refl's	5543	4549	7689	6102
Refl's I≥2 σ(I)	5047	3563	6284	4540
R_{int}	0.0550	0.0316	0.0504	0.0790
Parameters	300	382	478	437
Restraints	0	4	15	8
Largest Peak	0.648	0.259	2.451	1.005
Deepest Hole	-0.451	-0.265	-0.958	-0.935
GooF	1.050	1.059	1.059	1.044
wR_2 (all data)	0.0509	0.1547	0.1076	0.1821
wR_2	0.0497	0.1460	0.1019	0.1674
R_1 (all data)	0.0247	0.0672	0.0588	0.0889
R_1	0.0208	0.0527	0.0441	0.0650

Table S2 Selected bond lengths (Å) and angles (°) for **2**.

Cd1–O1	2.488(3)	O2–Cd1–O1	55.10(10)	O3–Cd2–O7^{2}	145.49(10)
Cd1–O2	2.272(3)	O2–Cd1–O5^{i}	159.40(11)	O4–Cd2–O3	55.11(10)
Cd1–O5^{i}	2.390(3)	O2–Cd1–O6^{i}	144.61(11)	O4–Cd2–O7^{2}	92.24(10)
Cd1–O6^{i}	2.322(3)	O2–Cd1–O9	90.08(12)	O4–Cd2–O8^{2}	145.70(10)
Cd1–O9	2.318(3)	O2–Cd1–O10	82.07(10)	O4–Cd2–O13	129.88(11)
Cd1–O10	2.379(3)	O2–Cd1–O11	86.79(12)	O8^{2}–Cd2–O3	158.20(11)
Cd1–O11	2.375(3)	O5^{i}–Cd1–O1	144.79(10)	O8^{2}–Cd2–O7^{2}	53.50(10)
Cd2–O3	2.444(3)	O6^{i}–Cd1–O1	89.83(10)	O8^{2}–Cd2–O13	84.13(11)
Cd2–O4	2.330(3)	O6^{i}–Cd1–O5^{i}	55.95(10)	O12–Cd2–O3	87.66(11)
Cd2–O7^{ii}	2.528(3)	O6^{i}–Cd1–O10	133.14(10)	O12–Cd2–O4	92.81(11)
Cd2–O8^{ii}	2.344(3)	O6^{i}–Cd1–O11	94.16(11)	O12–Cd2–O7^{2}	82.71(10)
Cd2–O12	2.290(3)	O9–Cd1–O1	88.37(11)	O12–Cd2–O8^{2}	85.07(11)
Cd2–O13	2.371(3)	O9–Cd1–O5^{i}	86.18(12)	O12–Cd2–O13	98.42(11)
Cd2–O14	2.258(3)	O9–Cd1–O6^{i}	93.79(11)	O13–Cd2–O3	76.64(10)
O2–Cd1–O1	55.10(10)	O9–Cd1–O10	88.49(11)	O13–Cd2–O7^{2}	137.49(10)
O2–Cd1–O5^{i}	159.40(11)	O9–Cd1–O11	170.17(11)	O14–Cd2–O3	97.88(13)
O2–Cd1–O6^{i}	144.61(11)	O10–Cd1–O1	137.03(10)	O14–Cd2–O4	86.24(12)
O2–Cd1–O9	90.08(12)	O10–Cd1–O5^{i}	77.59(10)		90.08(12)
O2–Cd1–O10	82.07(10)	O11–Cd1–O1	97.43(11)		82.07(10)
O2–Cd1–O11	86.79(12)	O11–Cd1–O5^{i}	93.49(12)		86.79(12)
O5^{1}–Cd1–O1	144.79(10)	O11–Cd1–O10	81.86(10)		144.79(10)

Symmetry codes: ^{i} -x, -y, 1-z; ^{ii} 1-x, 2-y, -z.

Table S3 Selected bond lengths (Å) and angles (°) for **3**.

Cd1–O5	2.408(14)	O5–Cd1–O5^{i}	71.4(6)	O1–Cd3–O1^{ii}	79.0(5)
Cd1–O7	2.432(14)	O5–Cd1–O7	95.1(5)	O2–Cd3–O1	54.0(4)
Cd1–O8	2.323(10)	O5–Cd1–O7^{i}	163.4(4)	O2–Cd3–O1^{ii}	107.4(5)
Cd1–O12	2.345(14)	O7–Cd1–O7^{i}	96.5(6)	O2–Cd3–O2^{ii}	88.5(7)
Cd2–O3	2.253(11)	O8–Cd1–O5^{i}	128.0(6)	O3–Cd3–O1^{ii}	162.6(5)
Cd2–O10	2.15(4)	O8–Cd1–O5	78.9(5)	O3–Cd3–O1	99.2(4)
Cd2–O11	2.236(14)	O8^{1}–Cd1–O7	117.6(5)	O3–Cd3–O2	84.5(4)
Cd2–O12^{iii}	2.411(19)	O8–Cd1–O7	55.2(5)	O3–Cd3–O2^{ii}	140.9(4)
Cd3–O1	2.443(11)	O8–Cd1–O8^{i}	87.8(5)	O3^{2}–Cd3–O2^{ii}	84.5(4)
Cd3–O2	2.365(15)	O8–Cd1–O12	134.2(3)	O3^{2}–Cd3–O2	77.3(5)
Cd3–O3	2.329(12)	O12–Cd1–O5	84.8(5)	O3–Cd3–O9	83.3(5)
Cd3–O9	2.33(2)	O12–Cd1–O7	84.4(4)	O9–Cd3–O1	79.4(5)
Cd4–O1	2.420(12)	O3–Cd2–O3^{ii}	80.5(6)	O9–Cd3–O2	128.8(4)
Cd4–O5	2.594(17)	O3–Cd2–O12^{iii}	86.7(4)	O1^{iv}–Cd4–O1^{v}	79.9(5)
Cd4–O6	2.296(12)	O10–Cd2–O3	91.1(6)	O1^{v}–Cd4–O5	76.5(5)
Cd4–O13	2.39(3)	O10–Cd2–O11	89.8(6)	O1^{iv}–Cd4–O5	117.5(4)
O1–C1	1.28(2)	O10–Cd2–O12^{iii}	177.0(8)	O5–Cd4–O5^{i}	65.6(5)
O2–C1	1.24(2)	O11–Cd2–O3^{ii}	87.6(6)	O6–Cd4–O1^{iv}	159.1(4)
O3–C22	1.274(19)	O11–Cd2–O3	168.1(6)	O6–Cd4–O1^{v}	79.5(4)
O4–C22	1.28(2)	O11–Cd2–O11^{ii}	104.3(10)	O6–Cd4–O5	53.7(4)
O5–C12	1.27(2)	O11–Cd2–O12^{iii}	92.1(5)	O6–Cd4–O5^{i}	110.4(4)
O6–C12	1.26(3)			O6^{1}–Cd4–O6	120.8(6)
O7–C30	1.23(2)			O6–Cd4–O13	93.1(6)
O8–C30	1.27(3)			O13–Cd4–O1^{v}	90.5(8)
				O13–Cd4–O5	145.7(4)

Symmetry codes: ^{i}2-x,+y,+z; ^{ii}1-x,+y,+z; ^{iii}-1/2+x,-1/2+y,+z; ^{iv}1/2+x,3/2-y,-1/2+z; ^{v}3/2-x,3/2-y,-1/2+z.

Table S4 Hydrogen bonding network in the crystal structure of H_4**L**.

#		$d_{D\cdots A}$ (Å)	$d_{H\cdots A}$ (Å)	$\alpha_{D-H\cdots A}$ (°)
d	O6^{i}–H6^{i}···O1	2.641(3)	1.79(6)	175(5)
e	O2–H2···O5^{ii}	2.604(3)	1.82(2)	160.3(2)
f	O8^{ii}–H8^{ii}···O3	2.589(3)	1.75(5)	170(6)
g	O4–H4···O7^{ii}	2.664(3)	1.84(6)	171(6)
h	C17–H17B···O1^{iii}	3.595(2)	2.750(18)	146.1(3)
i	C19–H19A···O5^{iii}	3.478(2)	2.687(14)	140.1(3)
j	C19–H19B···O2^{iv}	3.450(2)	2.766(15)	128.8(3)

Symmetry codes: ^{i} 1-x, -y, -z; ^{ii} 1-x, 2-y, 1-z; ^{iii} +x, 1+y, +z; ^{iv} 1-x, 1-y, -z.

Table S5 Intermolecular interactions found in compound **2**.

#		$d_{D\cdots A}$ (Å)	$d_{H\cdots A}$ (Å)	$\alpha_{D-H\cdots A}$ (°)
a	O9–H9A···O6	2.759(4)	1.97(3)	152.2(2)
b	O12–H12A···O4^{i}	2.693(4)	1.85(3)	174.2(2)
c	O15–H15A···O3	2.741(5)	1.98(3)	148.2(3)
d	O12–H12B···O10	2.783(4)	2.06(3)	142.6(2)
e	O10–H10A···O15	2.800(5)	2.00(4)	153.4(2)
f	O10–H10B···O8^{ii}	2.739(4)	2.04(3)	137.3(2)
g	O16^{i}–H16E^{i}···O12	2.970(5)	2.15(3)	162.8(3)
h	O14–H14A···O15^{iii}	2.687(5)	1.85(4)	165.6(3)
i	O14–H14B···O7^{iii}	2.710(5)	1.88(3)	165.3(3)
j	O11–H11A···O16^{iv}	2.841(5)	2.03(4)	157.7(2)
k	O11–H11B···O1^{v}	2.679(4)	1.85(3)	165.6(2)
l	O16^{iv}–H16D^{iv}···O2	2.775(5)	1.94(3)	166.4(3)
m	O9–H9B···O8^{vi}	3.032(5)	2.31(3)	142.3(2)

Symmetry codes: ^{i} 1-x, 2-y, -z; ^{ii} -x, 2-y, -z; ^{iii} 1+x, +y, +z; ^{iv} 1-x, 1-y, 1-z; ^{v} 1-x, -y, 1-z; ^{vi} -x, 1-y, 1-z.

Table S6 Intermolecular hydrogen bonds found in the crystal structure of compound **3**.

#		$d_{D\cdots A}$ (Å)	$d_{H\cdots A}$ (Å)	$\alpha_{D-H\cdots A}$ (°)
a	O9^{ii}–H9^{vi}···O5	2.825(19)	1.96(12)	155.4(8)
b	O11^{i}–H11A^{i}···O7^{v}	2.69(3)	1.92(14)	145.0(3)
c	O12–H12B^{v}···O4^{i}	2.672(13)	1.91(11)	148.9(13)
d	O10^{ii}–H10^{ii}···O2^{i}	2.75(2)	1.94(5)	157(13)

Symmetry codes according to Figure 3: ^{i} 3/2-x, 1/2+y, z; ^{ii} 3/2-x, 3/2-y, -1/2+z; ^{iii} 2-x, 2-y, -1/2+z; ^{iv} 3/2-x, 1/2+y, z; ^{v} 2-x, y, z; ^{vi} 1/2+x, 3/2-y, -1/2+z.

Table S7 Basis set effect on the τ angle, optimized at DFT level, and the absorption energy E_{abs}, wavelenght λ_{abs}, and oscillator strenght *f* calculated at TD-DFT level.[a]

	gas phase					DMSO solution				
Basis set	τ	E_{abs}	λ_{abs}[c]	*f*	λ_{em}	τ	E_{abs}	λ_{abs}[c]	*f*	λ_{em}
def2-SVP	26.00	4.162	297.9	0.842	450.2	21.62	4.089	303.2	1.257	468.2
def2-TZVP	26.88	4.126	300.5	0.912	–	21.75	4.025	308.0	1.344	–
6-31G	27.37	4.139	299.5	0.919	438.8	21.44	4.050	306.1	1.327	459.5
6-311G	27.50	4.120	300.9	0.907	445.3	22.06	4.028	307.8	1.368	468.1
6-311+G(d,p)	26.68	4.095	302.8	0.930	–	21.87	3.989	310.9	1.375	–

[a] PBE0 functional. [c] Experimental value λ_{abs} = 310 nm in DMSO, λ_{em} = 436 and 491 nm in DMSO and in the solid state, respectively.

Table S8 Adiabatic absorption energy E_{adia}, vertical transition energy $E^{GS-ES\#1}$, vertical transition wavelength $\lambda^{GS-ES\#1}$, emission energy E_{fluo}, and emission wavelength λ_{fluo} calculated at TD-DFT level (PBE0//def2-SVP) for H_4**L** in the gas phase and in DMSO. All energy values are given in eV and wavelengths in nm.

	gas	DMSO
$E_{adia}^{GS-ES\#1}$	3.3371	3.1846
$E^{GS-ES\#1}$	3.8685	3.7266
$\lambda^{GS-ES\#1}$	320.5	332.7
E_{fluo}	2.7543	2.6479
λ_{fluo}	450.2	468.2

Table S9 Transition vertical energy E_{abs} (eV) and corresponding wavelengths λ_{abs} (nm), oscillator strength *f* and main monoelectron transition contributions (larger than 20%) calculated for the lowest four excited states calculated for compound **4** in the gas phase at TD-DFT level (PBE0//def2-SVP).

Exc. State	#1	#2	#3	#4
E_{abs}	3.700	3.766	3.798	3.941
λ_{abs}	335.1	329.3	326.5	314.6
f	0.019	0.018	0.027	0.959
Excitations[a]	259→260 (71%)	258→260 (39%)	258→261 (60%)	258→260 (35%)
	259→261 (22%)	259→261 (36%)	258→262 (23%)	259→261 (32%)

[a] KS-HOMO = MO 259.